

# Immobilization of Fe, Mn and Co tetraphenylporphyrin complexes in MCM-41 and their catalytic activity in cyclohexene oxidation reaction by hydrogen peroxide

Andréia A. Costa<sup>a</sup>, Grace F. Ghesti<sup>a</sup>, Julio L. de Macedo<sup>a</sup>, Valdeilson S. Braga<sup>b</sup>,  
Marcello M. Santos<sup>a</sup>, José A. Dias<sup>a</sup>, Sílvia C.L. Dias<sup>a,\*</sup>

<sup>a</sup> Instituto de Química, Laboratório de Catálise, Universidade de Brasília, Caixa Postal 4478, Brasília, DF 70904-970, Brazil<sup>1</sup>

<sup>b</sup> Instituto de Ciências Ambientais e Desenvolvimento Sustentável, Universidade Federal da Bahia, Barreiras, BA 47805-100, Brazil

Received 16 October 2007; received in revised form 14 December 2007; accepted 17 December 2007

Available online 31 December 2007

## Abstract

Metalloporphyrin catalysts are able to carry out selective oxidation of organic substrates with several oxidizing agents. Recently, mesoporous materials have been studied as supports because they present high specific surface area, better dispersion and regeneration properties. This work presents the results of synthesis, characterization and application of three metalloporphyrin catalysts (FeTPPCL, MnTPPCL and CoTPP, where TPP = tetraphenylporphyrin) anchored on MCM-41, in the reaction of cyclohexene oxidation with hydrogen peroxide. A modified sol-gel preparation was chosen for the synthesis of the MCM-41 mesoporous material, as well as the anchoring was followed by Soxhlet extraction to ensure strong adsorption of the complex. The supported materials were much more stable than pure metalloporphyrins. The synthesized catalysts were characterized by UV-vis, FTIR, XRD, ICP-AES, <sup>29</sup>Si MAS-NMR and thermal analysis, before and after incorporation. Evidence of the metalloporphyrin immobilization was confirmed by elemental analysis and their activity in the oxidation reaction. FeTPPCL/MCM-41 showed higher conversion than CoTPP/MCM-41 and MnTPPCL/MCM-41. However, MnTPPCL/MCM-41 even in low concentration on the support showed a good conversion for the direct oxidation of cyclohexene with the highest turnover number ( $1.54 \times 10^5$ ). All catalysts showed similar selectivity that favors allylic oxidation products over epoxidation. No leaching of the metalloporphyrins was observed after the reaction.

© 2007 Elsevier B.V. All rights reserved.

**Keywords:** Metalloporphyrins; Molecular sieves; MCM-41; Cyclohexene oxidation; Hydrogen peroxide

## 1. Introduction

Nowadays, governmental projects and new legislations demand large investment in green chemistry procedures and environmental friendly technologies. One of the most interesting areas in catalysis is the development of inorganic-organic hybrid materials for catalytic oxidation reactions [1–5].

The selective oxidation of hydrocarbons and other organic compounds is still a challenge in chemical industries and academic field. Different types of metalloporphyrins and phthalocyanines have been largely studied for their ability in oxidation

reactions. New trends on catalysis preparations involve the immobilization of these molecules into molecular sieves to mimic biological systems like enzymes. An increasing understanding of enzymes behavior along with the growing need for catalysts that can activate aliphatic C–H bonds for selective oxidation have grown importance on biological systems with synthetic or biomimetic analogs [2,6,7].

Several systems containing supported macromolecules have been reported in literature. Among them, metalloporphyrin complexes present an important role in the field of oxidation reactions due to their inherent properties, and because many natural products contain similar groups (e.g., heme group, chlorophyll, vitamin B<sub>12</sub>, etc.) [8]. In the aim to achieve more stabilized and active systems, a number of supports have been tested. Nakagaki et al. [9,10] reported the incorporation of metalloporphyrins into porous vycor glass and zeolites, and studied their activity in the oxidation reactions of cyclohexane

\* Corresponding author. Tel.: +55 61 3307 2162; fax: +55 61 3368 6901.

E-mail addresses: [vsbraga@ufba.br](mailto:vsbraga@ufba.br) (V.S. Braga), [scdias@unb.br](mailto:scdias@unb.br) (S.C.L. Dias).

<sup>1</sup> <http://www.unb.br/iq/labpesq/qi/labcatalse.htm>.

and cyclohexene. Poltowicz and Haber extended the study by immobilization of metalloporphyrins on silica gel, polystyrene, montmorillonite K-10 and zeolite NaX showing that the support influences on the yield and selectivity of the products [11].

MCM-41 (Mobil Composition of Mater) is a molecular mesoporous sieve that has arisen as a new material for heterogeneous catalysis, with uniform pore size, high surface area and high capacity of adsorption [12–16]. These properties provide a wide variety of applications, especially when mechanical and chemical stabilities are required. The large pores and high amount of silanol groups of MCM-41 enhance its ability to immobilize macromolecules, such as metalloporphyrins. Recently, several authors have reported the application of macromolecules supported on MCM-41. Kulkarni and co-workers studied the immobilization of iron-porphyrin complexes inside the pores of MCM-41 using various synthetic procedures [17]. Nur and co-workers assigned that the ordered structure of MCM-41 may contribute to a high selectivity in the oxidation of benzene to phenol using an iron-porphyrin encapsulated catalyst [18]. Other authors established the high efficiency of these materials, showing their potential as active catalysts in oxidation reactions [2,8,19,20].

The work reported here presents the results of synthesis, characterization and application of three metalloporphyrin catalysts (FeTPPCL, MnTPPCL and CoTPP, where TPP = tetraphenylporphyrin) anchored on MCM-41 in the reaction of cyclohexene oxidation with  $H_2O_2$ . The synthesized catalysts were characterized by UV–vis, FTIR, XRD, ICP-AES,  $^{29}Si$  MAS-NMR and thermal analysis (TG/DTG), before and after incorporation on MCM-41.

## 2. Experimental

### 2.1. Synthesis of MCM-41

MCM-41 was synthesized as reported previously [14,21] with some modifications. In a 3 l round bottom flask, 510 ml of  $NH_4OH$  (Vetec) were mixed with 675 ml of Quartex water. To this mixture, 18.25 ml of cetyltrimethylammonium chloride (CTAC, Aldrich) was added under mild conditions (30–35 °C) and constant magnetic stirring. After a few minutes, 25 ml of tetraethylorthosilicate (TEOS, Aldrich) were added dropwise. After 2 h, the resulting product was filtered and washed with Quartex water until it was chloride free ( $AgNO_3$  test). The material was dried and calcined at 550 °C for 5 h (10 °C  $min^{-1}$ ) in a muffle furnace (model 3P-S, EDG Equipments). The molar ratio of the Si-MCM-41 synthesis was 525( $H_2O$ ):69( $NH_4OH$ ):0.125(CTAC):1(TEOS).

### 2.2. Preparation of ligand and the complexes

The procedure used for porphyrin preparation was based on Adler's method [22]. 8 ml of freshly distilled pyrrol, 350 ml of propionic acid and 12 ml of benzaldehyde were added to a flask, and the solution was kept under reflux conditions for 30 min. After the reaction, the free base meso-tetraphenylporphyrin (TPP) was filtered and repeatedly washed with methanol and

hot water. Finally, the solid was purified by a sublimation technique using a horizontal furnace, where single needle crystals of TPP were obtained [22].

The metalation procedure was followed as well, with some modifications [23]. The purified TPP was allowed to reflux, with a small excess of the metal chlorides (molar ratio of 1:3) in 45 ml of dimethylformamide. After 4 h of reflux and 2 h of ice bath, 45 ml of cold water was added and an immediate precipitation of the solid occurred. The structure of the complexes was confirmed by FTIR, UV–vis and  $^1H$  NMR.

### 2.3. Preparation of catalysts

In order to immobilize the complexes within the MCM-41, 0.2 g of metalloporphyrin (FeTPPCL, MnTPPCL or CoTPP) in dichloromethane were slowly added to 2 g of MCM-41 in 50 ml of dichloromethane. The mixture was kept under magnetic stirring for 48 h, and then under reflux conditions for 1 h. The solid product was then washed in a Soxhlet apparatus for 48 h with 300 ml of dichloromethane, in order to remove the weakly adsorbed metallocomplexes on the mesoporous surface. Finally, the shallow-green solids were dried in air at room temperature.

### 2.4. Oxidation reactions

Oxidation reactions were carried out at atmospheric pressure under reflux conditions mixing 10 mmol of cyclohexene, 12 mmol of oxidizing agent ( $H_2O_2$ ), 0.1 g of the catalyst and 3 ml of acetonitrile [8]. At first, solvent, substrate and catalyst were introduced into the reaction flask followed by stirring. After a few minutes, the oxidant agent was slowly added to the reaction. The solid was filtered after 8 h, and the solution was then submitted to chromatographic analysis. GC-FID (GC-17A, Shimadzu) with CBP1-PONA column (50 m  $\times$  0.15 mm  $\times$  0.42  $\mu m$ ) was used to determine the cyclohexene conversion and GC-MS (QP5050A, Shimadzu, same column type) was used to identify the reaction products.

### 2.5. Catalysts characterization

#### 2.5.1. UV–vis

UV–vis spectra were obtained on a Thermo Spectronic spectrophotometer model Genesys 10UV, from 300–700 nm using 1 cm quartz cuvette.

#### 2.5.2. FTIR

FTIR spectra were recorded on a Bomen–Hartman & Braun, Michelson MB-100 spectrometer. The measurements were performed using KBr pellets (128 scans with a 4  $cm^{-1}$  resolution).

#### 2.5.3. $^{29}Si$ magic angle spinning (MAS)-NMR

NMR experiments were performed at 7.05 T with a Varian Mercury Plus NMR spectrometer equipped with a 7 mm Varian probe and zirconia rotors.  $^{29}Si$  MAS spectra were recorded at a speed of 3 kHz, pulse duration of 7.5  $\mu s$  ( $\pi/2$ ), a recycle delay of 20 s, and 500 scans were acquired for each spectrum. The spectra were external referenced to kaolin (−91.5 ppm). MAS-

NMR data were deconvoluted using a Gaussian mathematical fit.

#### 2.5.4. Thermal analysis

TG/DTG curves were obtained in a 2960 Simultaneous DSC-TGA (TA Instruments) using synthetic air (99.999%) as purge gas (100 ml min<sup>-1</sup>). The analyses were made from ambient temperature (~26 °C) up to 900 °C at 10 °C min<sup>-1</sup>, and  $\alpha$ -Al<sub>2</sub>O<sub>3</sub> was used as reference material.

#### 2.5.5. X-ray diffraction analysis

The XRD analysis was made at 2° min<sup>-1</sup> with a Rigaku diffractometer, model D/MAX-2A/C with radiation Cu K $\alpha$  at 40 kV and 20 mA.

#### 2.5.6. Elemental analysis

The amount of adsorbed metalloporphyrin in the mesoporous molecular sieves of MCM-41 was determined by atomic emission spectroscopy with inductive coupled plasma (ICP-AES, Spectroflame-FVMØ3). The samples were digested by a traditional acid method (HF, HNO<sub>3</sub>, HClO<sub>4</sub> and HCl), diluted adequately and analysed for Fe, Mn and Co [24].

### 3. Results and discussion

#### 3.1. Characterization of the complexes

Iron, manganese and cobalt were chosen as metal centers to the metalloporphyrin complexes due to their reported oxidation properties [11,25]. The synthetic procedure for metalloporphyrins preparation is widely known and the metal complexes were easily obtained [22,23].

UV–vis and FTIR spectroscopies were used to evidence the formation of the complexes. UV–vis absorption measurements for all the complexes were in agreement with the literature values (Table 1) [26]. In addition to this, FTIR measurements of the free base porphyrin and their respective complexes of iron, manganese and cobalt show some characteristic bands that are directly related with the obtained metalloporphyrins: (a) the absence of the band at 3300 cm<sup>-1</sup>, which is related to N–H stretching in the metal complexes spectra, indicates that the intramolecular hydrogen bonds usually present in the free base porphyrin do not exist after metal complexation; (b) the increase in the intensity of the bands at ~1350 cm<sup>-1</sup>, related to C=N stretching [27]; (c) the displacement of the intense band near to 1000 cm<sup>-1</sup> to higher wavenumbers is a strong

Table 1  
Experimental and theoretical (literature) values for Soret bands obtained by UV–vis analysis

Metalloporphyrin	Soret band maximum (nm)	
	Experimental	Literature <sup>a</sup>
FeTPPCL	417	418
CoTPP	408 and 526	409 and 524
MnTPPCL	583 and 619	583 and 618

<sup>a</sup> Obtained from reference [26].

evidence of the metalloporphyrin complexes formation and stability.

#### 3.2. Characterization of the support

X-ray diffraction (XRD) analyses of the synthesized mesoporous material revealed the typical three peak pattern of the MCM-41, with a strong reflection at 2.4° (100), and two others with low intensity at 4.2° (110) and 4.7° (200). A study reported by Cai and co-workers [14] shows that the highly ordered hexagonal channel array of these materials are strongly dependent of the molar ratio water/template. In the present work, an ideal value of 4200 (H<sub>2</sub>O:CTAC), as suggested by Cai, was used to prepare a well-ordered MCM-41 material.

FTIR spectrum of as synthesized MCM-41 clearly shows that the bands related to the carbon long chain template molecules were removed after the thermal treatment. The absence of bands around 3200 and 1400 cm<sup>-1</sup> indicates that the activation of the support was effective for the formation of a free template bidimensional structure, where the silanol groups are available to anchor the metalloporphyrin complexes. [Supplementary data](#) are provided for the characterization of the complexes and the support.

#### 3.3. Synthesis of heterogenised metalloporphyrins

Among various methods employed to incorporate metal complexes inside the pores of molecular sieves, meso-tetraphenylporphyrins of iron, cobalt and manganese were immobilized through an anchoring method. Since MCM-41 mesoporous materials have pore sizes larger than 20 Å, the direct encapsulation of metalloporphyrins inside the mesoporous material can be achieved [17]. The amount of metalloporphyrin on the support was determined by elemental analysis (ICP-AES), and the results showed as percentages (mass%:mass%) are depicted in Table 2.

The catalysts were prepared on a ratio of 1:10 (metalloporphyrin/support) and functionalization was not performed either on the support or in the complex. Although similar washings were carried out with the Soxhlet system in each case, it could be observed different results for iron, cobalt and manganese porphyrins incorporation. This is related to the interaction of each complex with the MCM-41.

FTIR spectra (Fig. 1) were obtained in order to observe the interactions between silanol groups on the surface support and metalloporphyrin complexes. The bands observed at 475, 800, 960 and 1098 cm<sup>-1</sup>, which are related to  $\delta$ (Si–O–Si),  $\nu_s$ (Si–O–Si),  $\nu$ (Si–OH) and  $\nu_{as}$ (Si–O–Si), respectively, are the

Table 2  
ICP-AES results for the metals after metalloporphyrins immobilization

Complex	Amount anchored on MCM-41 (mass%)
MnTPPCL	0.14
FeTPPCL	2.06
CoTPP	5.42

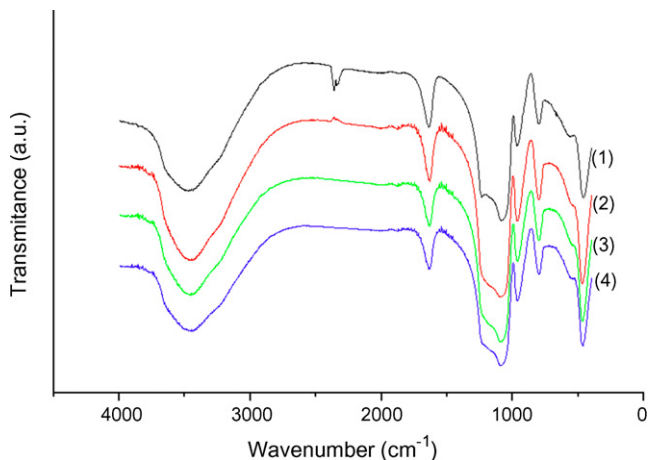


Fig. 1. FTIR spectra of synthesized catalysts at room temperature: (1) MCM-41; (2) CoTPP/MCM-41; (3) FeTPP/MCM-41; (4) MnTPP/MCM-41.

main features of MCM-41 [21]. Although slight changes could be observed at 1000 and 1200  $\text{cm}^{-1}$ , the band assigned around 950  $\text{cm}^{-1}$  is the one that indicates the presence of organic groups on the MCM-41 surface [18] by a shift to lower wavenumbers. Due to the low amount of metalloporphyrins anchored on the surface support, this main characteristic of the immobilized complexes could not be observed.

$^{29}\text{Si}$  MAS-NMR spectra elucidated better the interactions between the complexes and the support. After careful deconvolution of NMR data, it was possible to obtain the relative areas of each peak and thus calculate important parameters for the studied materials, such as condensation degree [28], relative proportion of different silicon environments [29] and molar percentage of silanol groups [15].

In all cases, it was verified changes on MCM-41 silicon environments after complex immobilizations. The chemical shifts related to  $Q^4$ ,  $Q^3$  and  $Q^2$  environments, i.e.  $\text{Si}(4\text{Si})$ ,  $\text{Si}(3\text{Si}, 1\text{OH})$  and  $\text{Si}(2\text{Si}, 2\text{OH})$ , respectively, were observed at ca.  $-105$ ,  $-95$  and  $-86$  ppm.

Calcination procedures of MCM-41 naturally lead to an increase of  $Q^4$  environment due to the condensation of

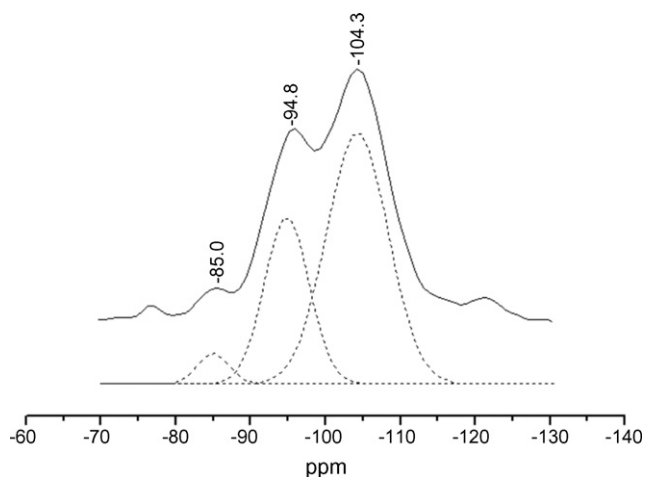


Fig. 2.  $^{29}\text{Si}$  MAS-NMR result for MCM-41 calcinated at 550  $^{\circ}\text{C}/5$  h/air.

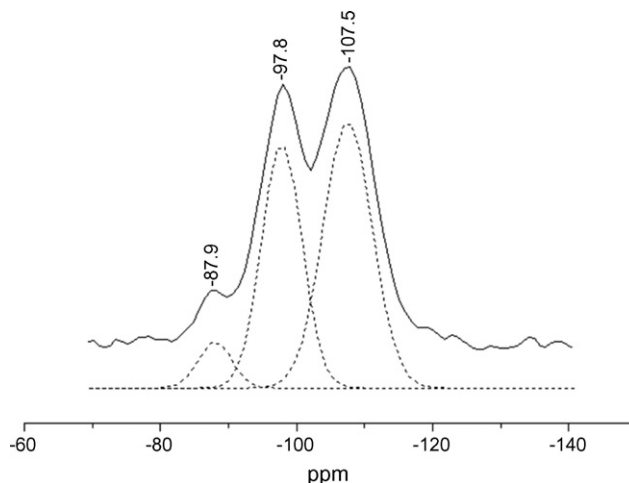


Fig. 3.  $^{29}\text{Si}$  MAS-NMR result for MCM-41 calcinated at 550  $^{\circ}\text{C}/5$  h/air, treated with  $\text{CH}_2\text{Cl}_2$  and dried at room temperature.

silanol groups and formation of siloxane in the structure (Eq. (1)). Figs. 2–6 show that the relative chemical environments were clearly affected by complex immobilizations. Analyzing Tables 2 and 3, one can observe that an increase in metalloporphyrin amount leads to a decrease in the molar percentage of silanol groups. Considering that the condensation degree parameter allows a correlation between the relative chemical environments of the samples, it can be seen that the interaction between metalloporphyrins and the support leads to a pseudo  $Q^4$  environment. This occurs because the interaction between metalloporphyrin and silanol groups generates modified  $Q^3$  environment, which are computed as  $Q^4$  environments (Fig. 7). According to Table 3, there is a considerable increase in  $Q^4$  values that corroborates the above statement.



Considering that catalyst applications are dependent on the thermal properties [30], thermal analyses were also used to verify the stability of the complexes and the supported catalysts designed for oxidation reactions. The thermal behavior of MCM-41 has

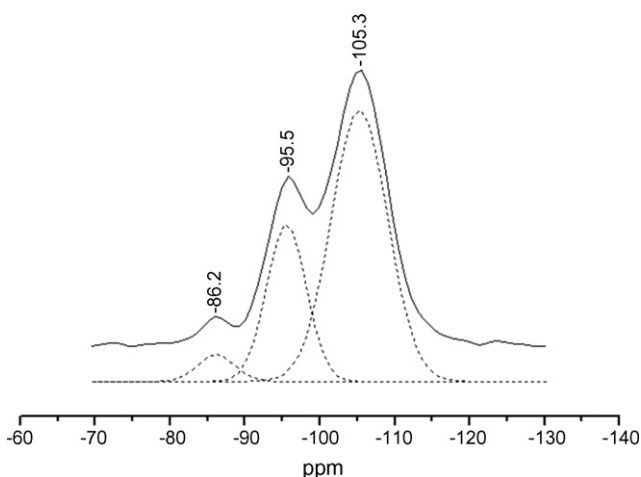


Fig. 4.  $^{29}\text{Si}$  MAS-NMR result for FeTPP supported on MCM-41.

Table 3  
Relative proportion areas of  $^{29}\text{Si}$  MAS-NMR peaks related to the different silicon chemical environments

Samples	Relative proportion of the chemical environment				
	$Q^2$	$Q^3$	$Q^4$	$(Q_3 + Q_2)/Q_4^a$	SiOH (mol%-Si) <sup>b</sup>
MCM-41 ( $\text{CH}_2\text{Cl}_2$ )	1	3	4	0.9	64.6
MnTPPCL/MCM-41	1	4	8	0.7	45.3
FeTPPCL/MCM-41	1	4	10	0.5	36.6
CoTPP/MCM-41	1	5	15	0.4	34.7

<sup>a</sup> Condensation degree [28].

<sup>b</sup> Amount of silanol groups relative to total Si =  $[(2 Q_2 + Q_3)/(Q_2 + Q_3 + Q_4)] \times 100\%$  [15].

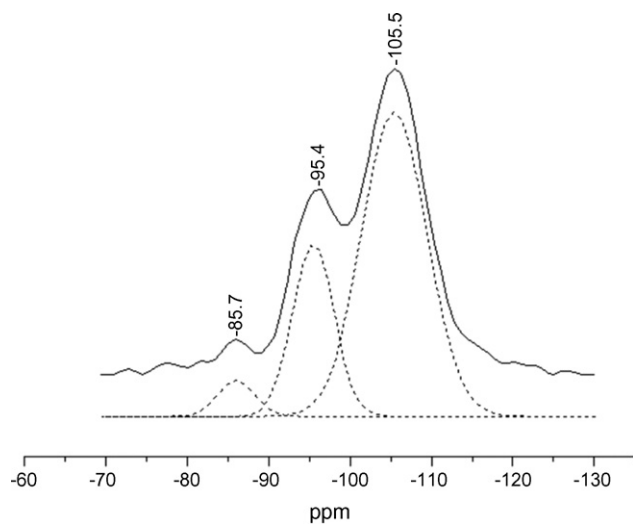


Fig. 5.  $^{29}\text{Si}$  MAS-NMR result for CoTPP supported on MCM-41.

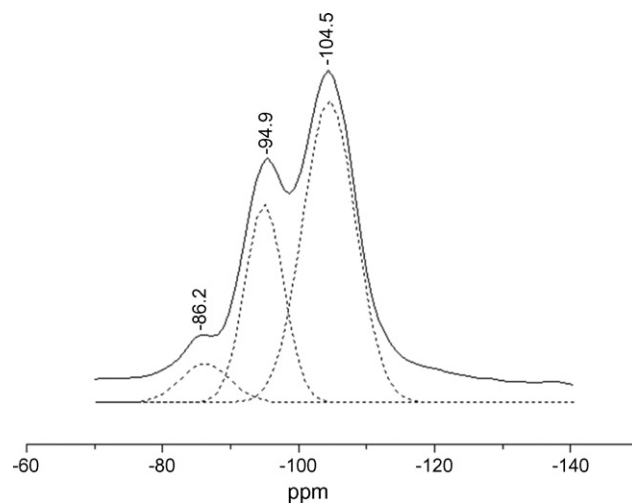


Fig. 6.  $^{29}\text{Si}$  MAS-NMR result for MnTPPCL supported on MCM-41.

been investigated and it presents a mass loss in the range from 25 to 950 °C, related to the dehydration followed by dehydroxylation of silanol groups [15].

Further investigation using TG/DTG and DTA curves (Table 4) showed that the catalysts of FeTPPCL, CoTPP and MnTPPCL are stable up to 256, 293 and 352 °C, respectively. The initial mass loss (from 1 up to 3%) for the metalloporphyrin complexes is related to adsorbed water and small impurities on the structure, such as, free ligand, pyrrol, etc. The partial mass losses, related to the decomposition stages (I, II and III in Table 4), are associated to the sequential thermal degradation of the porphyrin macrocycles. The different thermal behavior observed for these samples is associated to the distinct metal centers. Wei et al. [30] showed that the thermal decomposition reaction rate of the porphyrin at the same temperature is greatly

affected by the incorporation of a metal center. The formation of metal oxide residues is observed after the complete decomposition of the macrocycle (ca. 87%). All mass losses determined experimentally were in agreement with the calculated theoretical values.

After impregnation on MCM-41, an increase on the decomposition temperature was observed (Figs. 8–10). For iron immobilized complex, the initial decomposition changed from 256 to 350 °C after immobilization. This process produced an increase of almost 100 °C on the stabilization of the complex. Similar behavior was observed for manganese (increase of 168 °C), and for cobalt complex after impregnation there was no mass loss above 200 °C. In fact, a second mass loss below 200 °C was observed only for the immobilized cobalt complex. This can be related to the stabilization of the complex after the interaction between the metal and the OH silanol group of MCM-

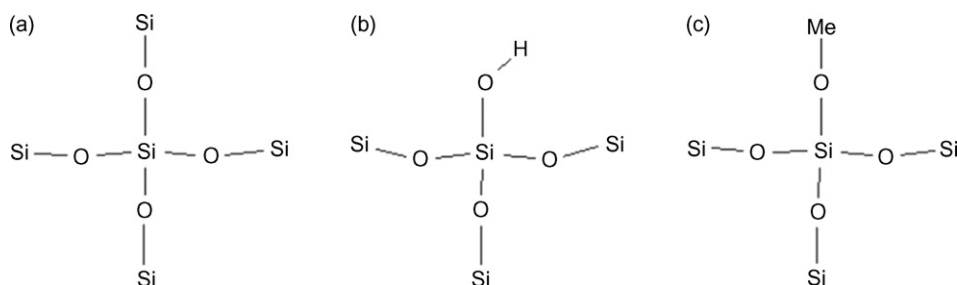


Fig. 7.  $^{29}\text{Si}$  MAS-NMR  $Q_4$  (a),  $Q_3$  (b) and  $Q_4$  simulated (c), where Me is the metalloporphyrin.



Table 4  
Thermal decomposition of metalloporphyrin complexes

Sample	Stage: $\Delta T$ ( $^{\circ}\text{C}$ )	DTG ( $^{\circ}\text{C}$ )	DTA <sup>a</sup> ( $^{\circ}\text{C}$ )	Mass loss (%)			Residue
				Partial	Initial	Total	
MnTPPCI	I: 352–478	437; 443	432; 444	22.1	1.8	87.3	Mn <sub>3</sub> O <sub>4</sub>
	II: 478–583	549; 565	545	65.2			
FeTPPCI	I: 256–404	354; 394	391	25.5	2.9	86.6	Fe <sub>3</sub> O <sub>4</sub>
	II: 404–492	424; 456	421; 448	61.1			
CoTPP	I: 293–479	442; 463	453	34.0	1.0	88.7	Co <sub>3</sub> O <sub>4</sub>
	II: 479–511	499	498	15.0			
	III: 511–585	573	555	39.7			

<sup>a</sup> All peaks are exothermic.

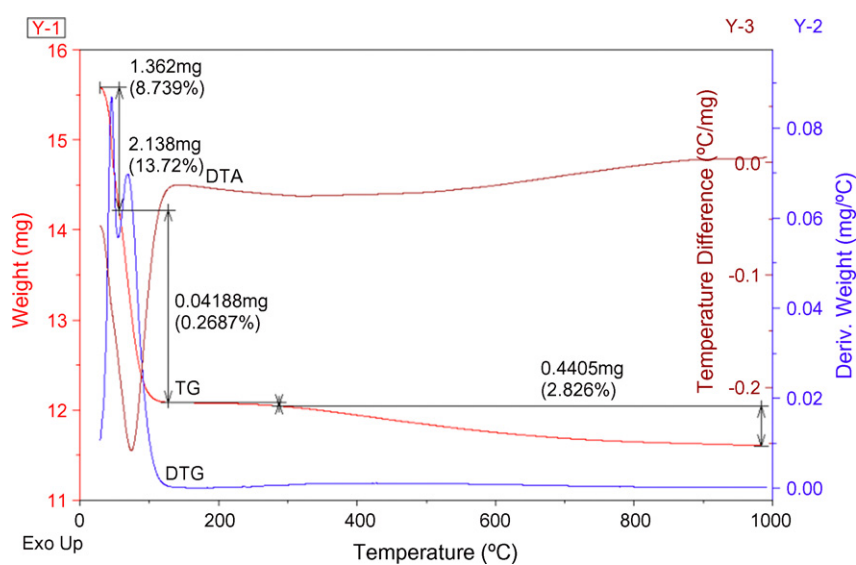


Fig. 8. TG/DTG and DTA curves for CoTPP/MCM-41.

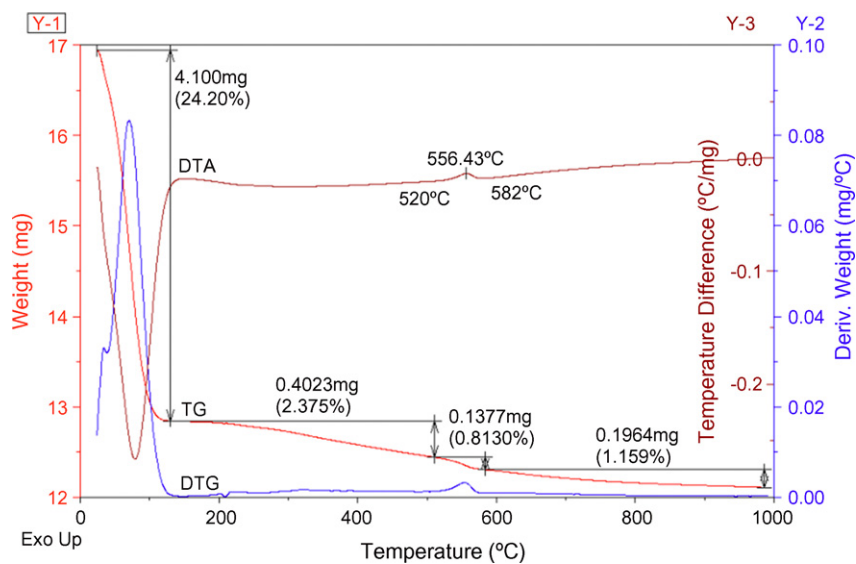


Fig. 9. TG/DTG and DTA curves for MnTPPCI/MCM-41.

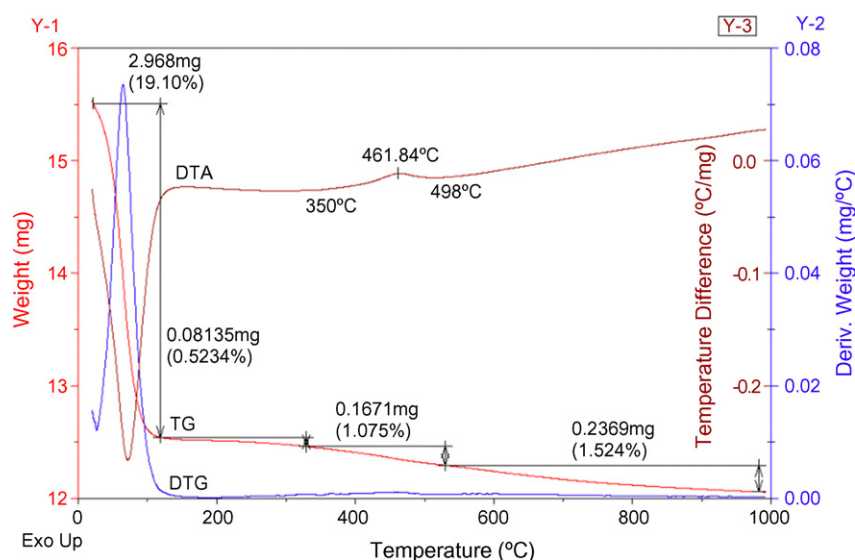


Fig. 10. TG/DTG and DTA curves for FeTPPCI/MCM-41.

41. Among the three metals, cobalt would present the weakest interaction while manganese would present the strongest interaction, based on hard–soft acid–base, according to the following series of hardness:  $\text{Co(II)} < \text{Fe(III)} < \text{Mn(III)}$ .

#### 3.4. Oxidation reactions

Selective oxidations of hydrocarbons under mild conditions have great academic interest and industrial value [19]. A number of oxidation systems that mimic cytochrome P-450 using iron, manganese and cobalt metalloporphyrins have already been reported [25]. Recent results show that metalloporphyrin complexes immobilized into zeolite channels present particular properties due to the isolation of active sites, avoiding catalyst self-deactivation through dimerization. In addition, the heterogeneization of these complexes is a way to protect them from the oxidative reaction media [3,4,8,11]. After the reaction, the systems were tested for leaching of the metalloporphyrins. No metal was detected in the solutions, which confirms the efficiency of the procedure for incorporation of metalloporphyrins into MCM-41.

Hydrogen peroxide was chosen in this work as a clean oxidant agent, since the use of non-expensive and environmental friendly reactants (e.g., molecular oxygen, alkyl peroxides) are very important in modern catalysis. Moreover, hydrogen peroxide molecules generate water as by product, showing its biological value [31].

The results of catalytic cyclohexene conversion by iron, manganese and cobalt metalloporphyrins encapsulated into MCM-41 mesopores are described in Table 5. In order to compare the results, two blank experiments were performed. Blank 1 consisted of the oxidant agent and blank 2 was composed of the oxidant agent and pure MCM-41. These systems were studied to confirm the complex activities in the reaction. A very low amount of substrate was converted in the blank reactions, showing that the supported metalloporphyrin complexes are the active centers for cyclohexene oxidation reaction.

Data of catalytic oxidation reactions of cyclohexene with  $\text{H}_2\text{O}_2$ , selectivity and turnover numbers (TON) are presented in Table 6. All studied catalysts showed a remarkable activity on cyclohexene oxidation reactions. Although FeTPPCI/MCM-41 showed the highest conversion compared to Co and Mn catalysts, the MnTPPCI/MCM-41 catalyst, even in low concentration on the support, was the most active in the direct oxidation of cyclohexene, in agreement to literature [25]. Although under adverse conditions, CoTPP/MCM-41 showed a good activity in the cyclohexene oxidation reaction, since it is mainly active in one-electron redox processes (e.g., activation of dioxygen); whereas Mn and FeTPP/MCM-41 show similar properties and are able to activate single oxygen donors (such as hydrogen peroxide) in a two-electron redox process [25].

The selectivity of products for alkene oxygenation mechanism is dependent of several parameters (e.g., reaction conditions, porphyrin structure, central cation, solvent, oxidant agent, co-catalyst). The formation of two oxidizing intermediates (hydroperoxy- and oxo-species) from the interaction of metalloporphyrin with  $\text{H}_2\text{O}_2$  has been proposed in literature [32–34]. Rebelo et al. [34] showed that the selectivity of metalloporphyrin catalysts depends on the formation of these two intermediate species. The mechanism proposed involves at first, the formation of hydroperoxy-species, followed by either

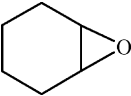
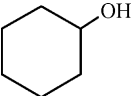
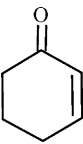
Table 5  
Results of cyclohexene oxidation reactions

Catalyst	Cyclohexene Conversion (%)
Blank <sup>a</sup>	1.0
MCM-41 <sup>b</sup>	8.2
FeTPPCI/MCM-41	25.8
CoTPP/MCM-41	11.8
MnTPPCI/MCM-41	15.3

<sup>a</sup> Reaction condition: 12 mmol of  $\text{H}_2\text{O}_2$ , 10 mmol of cyclohexene and 3 ml of acetonitrile.

<sup>b</sup> Reaction condition: 0.1 g of MCM-41, 12 mmol of  $\text{H}_2\text{O}_2$ , 10 mmol of cyclohexene and 3 ml of acetonitrile.

Table 6  
Catalytic behavior of metalloporphyrin complexes anchored on MCM-41

Supported catalyst	Fe	Mn	Co
Conversion (%)	25.8	15.3	11.8
Selectivity (%)			
	25.9	20.1	23.9
	46.0	46.0	39.0
	28.1	33.9	37.1
TON <sup>a</sup>	$1.76 \times 10^4$	$1.54 \times 10^5$	$2.93 \times 10^3$

<sup>a</sup> TON = mmol of the products to mmol of metal content on the catalyst.

the oxygen transfer to the substrates or the development of highly active oxo-species. Indeed, the use of protic solvents and iron as central cation in the absence of co-catalyst favors hydroperoxy-species, meanwhile the use of aprotic solvents, manganese (central cation) in the presence of co-catalyst favors oxo-species.

The selectivity pattern (cyclohexenone and cyclohexanol) suggests that the metalloporphyrins were mostly anchored on the internal pore wall surface of MCM-41. According to Zimowska et al. [3], porphyrin species anchored on the internal pore wall are more selective for cyclohexanol and cyclohexenone than epoxidation products. A favorable orientation of the cyclohexene molecule and the anchored metalloporphyrin complex in order to form the epoxide intermediate becomes restricted within the MCM-41 channels. Thus, epoxidation products are favorable through external surface impregnation of the complexes. These results are in agreement with literature data, in which the efficiency of the process is controlled mainly by the diffusion of reagents and products into the mesopores of the support [2].

#### 4. Conclusions

The present work showed the results of synthesis, characterization and application of three metalloporphyrin catalysts (FeTPPCI, MnTPPCI and CoTPP) anchored on MCM-41, in the oxidation reaction of cyclohexene with hydrogen peroxide. The adopted strategy to obtain the catalysts suggests that these materials appear as good catalysts for the reported oxidation reaction. <sup>29</sup>Si MAS-NMR and FTIR studies showed that the interaction between the metalloporphyrins and the support leads to modifications in MCM-41 chemical environment, and an increase in metalloporphyrin amount leads to a decrease in the molar percentage of silanol groups due to its direct interaction. Thermal analysis was also used to study the complexes and the supported catalysts, and the results indicate that the thermal

stability is directly affected by the metal center and an increase on the stability is observed after anchoring.

FeTPPCI/MCM-41 presented the highest conversion (25.8%) and MnTPPCI/MCM-41 was the most active catalyst in the direct oxidation of cyclohexene (TON =  $1.54 \times 10^5$ ). The distribution of the oxidation products (cyclohexenone and cyclohexanol) indicates that the porphyrin species were anchored on the internal pore surface of MCM-41. No leaching of metalloporphyrins was observed after the reaction.

#### Acknowledgments

We acknowledge CNPq for scholarships to doctorate students (A.A. Costa and G.F. Ghesti) and the financial support provided by UnB-IQ (FUNPE), FINATEC, FINEP/CTPetro, FINEP/CTInfra, and MCT/CNPq. The authors would like to thank Professors Edi Mendes Guimarães from Laboratório de Difração de Raios-X and Geraldo Boaventura from Laboratório de Geoquímica (IG/UnB) for XRD and ICP-AES measurements.

#### Appendix A. Supplementary data

Supplementary data associated with this article can be found, in the online version, at doi:10.1016/j.molcata.2007.12.024.

#### References

- [1] A. Maldotti, A. Molinari, G. Varani, M. Lenarda, L. Storaro, F. Bigi, R. Maggi, A. Mazzacani, G. Sartori, *J. Catal.* 209 (2002) 210–216.
- [2] J. Poltowicz, K. Pamin, L. Matachowski, E.M. Serwicka, R. Mokaya, Y. Xia, Z. Olejniczak, *Catal. Today* 114 (2006) 287–292.
- [3] M. Zimowska, A. Michalik-Zym, J. Poltowicz, M. Bazarnik, K. Bahranowski, E.M. Serwicka, *Catal. Today* 124 (2007) 55–60.
- [4] G. Huang, S. Liu, A. Wang, Y. Guo, H. Zhou, *Catal. Commun.* 8 (2007) 1183–1186.
- [5] F.L. Benedito, S. Nakagaki, A.A. Saczk, P.G. Peralta-Zamora, C.M.M. Costa, *Appl. Catal. A* 250 (2003) 1–11.
- [6] B. Meunier, *Chem. Rev.* 92 (1992) 1411–1456.
- [7] J. Haber, K. Pamin, J. Poltowicz, *J. Mol. Catal. A: Chem.* 224 (2004) 153–159.
- [8] F. Farzaneh, J. Taghavi, R. Malakooti, M. Ghandi, *J. Mol. Catal. A: Chem.* 244 (2005) 252–257.
- [9] S. Nakagaki, A.R. Ramos, F.L. Benedito, P.G. Peralta-Zamora, A.J.G. Zarbin, *J. Mol. Catal. A: Chem.* 185 (2002) 203–210.
- [10] S. Nakagaki, C.R. Xavier, A.J. Wosniak, A.S. Mangrich, F. Wypych, M.P. Cantão, I. Denicoló, L.T. Kubota, *Colloids Surf. A* 168 (2000) 261–276.
- [11] J. Poltowicz, J. Haber, *J. Mol. Catal. A: Chem.* 220 (2004) 43–51.
- [12] J.S. Beck, J.C. Vartulli, W.J. Roth, M.E. Leonowicz, C.T. Kresge, K.D. Schmitt, C.T.-W. Chu, D.H. Olson, E.W. Sheppard, S.B. McCullen, J.B. Higgins, J.L. Schlenke, *J. Am. Chem. Soc.* 114 (1992) 10834–10843.
- [13] A. Corma, *Chem. Rev.* 97 (1997) 2373–2420.
- [14] Q. Cai, W.-Y. Lin, F.-S. Xiao, W.-Q. Pang, X.-H. Chen, B.-S. Zou, *Microporous Mesoporous Mater.* 32 (1999) 1–15.
- [15] N. Igarashi, K.A. Koyano, Y. Tanaka, S. Nakata, K. Hashimoto, T. Tatsumi, *Microporous Mesoporous Mater.* 59 (2003) 43–52.
- [16] M. Luechinger, L. Frunz, G.D. Pirngruber, R. Prins, *Microporous Mesoporous Mater.* 64 (2003) 203–211.
- [17] V. Radha Rani, M. Radha Kishan, S.J. Kulkarni, K.V. Raghavan, *Catal. Commun.* 6 (2005) 531–538.
- [18] E.J. Nassar, Y. Messaddeq, S.J.L. Ribeiro, *Quim. Nova* 25 (2002) 27–31.
- [19] H. Nur, H. Hamid, S. Endud, H. Hamdan, Z. Ramli, *Mater. Chem. Phys.* 96 (2006) 337–342.



- [20] D. Brunel, N. Bellocq, P. Sutra, A. Cauvel, M. Laspéras, P. Moreau, F. Di Renzo, A. Galarneau, F. Fajula, *Coord. Chem. Rev.* 178 (1998) 1085–1108.
- [21] M.P. Souza, Thesis, Universidade de Brasília, Brazil, 2005.
- [22] A.D. Adler, F.R. Longo, J.D. Finarelli, J. Goldmacher, J. Assour, L. Korsakoff, *J. Org. Chem.* 32 (1967) 476.
- [23] A.D. Longo, F.R. Longo, F. Kampas, J. Kim, *J. Inorg. Nucl. Chem.* 32 (1970) 2443–2445.
- [24] A.A. Costa, Thesis, Universidade de Brasília, Brazil, 2006.
- [25] E.M. Serwica, J. Poltowicz, K. Bahranowski, Z. Olejniczak, W. Jones, *Appl. Catal. A* 275 (2004) 9–14.
- [26] J.E. Falk, *Porphyrins and Metalloporphyrins. Their General, Physical and Coordination Chemistry and Laboratory Methods*, Elsevier, New York, 1964.
- [27] A. Fuerte, A. Corma, M. Iglesias, E. Morales, F. Sánchez, *J. Mol. Catal. A: Chem.* 246 (2006) 109–117.
- [28] S. Shylesh, A.P. Singh, *J. Catal.* 244 (2006) 52–64.
- [29] V.M.S. Gil, C.F.G.C. Geraldés, *Ressonância Magnética Nuclear—Fundamentos, Métodos e Aplicações*, Fundação Calouste Gulbenkian, Lisboa, 1987.
- [30] X. Wei, X. Du, D. Chen, Z. Chen, *Thermochim. Acta* 440 (2006) 181–187.
- [31] F.S. Vinhado, P.R. Martins, A.P. Masson, D.G. Abreu, E.A. Vidoto, O.R. Nascimento, Y. Iamamoto, *J. Mol. Catal. A: Chem.* 188 (2002) 141–151.
- [32] I.D. Cunningham, T.N. Danks, J.N. Hay, I. Hamerton, S. Gunathilagan, *Tetrahedron* 57 (2001) 6847–6853.
- [33] T. Chen, E. Kang, G. Tan, S. Liu, S. Zheng, K. Yang, S. Tong, C. Fang, F. Xiao, Y. Yan, *J. Mol. Catal. A* 252 (2006) 56–62.
- [34] S.L.H. Rebelo, M.M. Pereira, M.M.Q. Simões, M.G.P.M.S. Neves, J.A.S. Cavaleiro, *J. Catal.* 234 (2005) 76–87.